



Optimum reaction ratio of coal fly ash to blast furnace cement for effective removal of hydrogen sulfide

Asaoka, Satoshi ; Okamura, Hideo ; Kim, Kyunghoi ; Hatanaka, Yuzuru ; Nakamoto, Kenji ; Hino, Kazutoshi ; Oikawa, Takahito ; Hayakawa, ...

(Citation)

Chemosphere, 168:384-389

(Issue Date)

2017-02

(Resource Type)

journal article

(Version)

Accepted Manuscript

(Rights)

©2017.

This manuscript version is made available under the CC-BY-NC-ND 4.0 license
<http://creativecommons.org/licenses/by-nc-nd/4.0/>

(URL)

<https://hdl.handle.net/20.500.14094/90003673>



Optimum reaction ratio of coal fly ash to blast furnace cement for effective removal
of hydrogen sulfide

Satoshi ASAOKA^{a*}, Hideo OKAMURA^a, Kyunghoi KIM^b,
Yuzuru HATANAKA^c, Kenji NAKAMOTO^d, Kazutoshi HINO^d,
Takahito OIKAWA^d, Shinjiro HAYAKAWA^e, Tetsuji OKUDA^f

a Research Center for Inland Seas, Kobe University

5-1-1 Fukaeminami, Higashinada, Kobe, 658-0022 JAPAN

b College of Environmental and Marine Sciences and Technology, Pukyong National
University

45, Yongso-ro, Nam-Gu, Busan 48513, KOREA

c Faculty of Maritime Sciences, Kobe University

5-1-1 Fukaeminami, Higashinada, Kobe, 658-0022 JAPAN

d The Chugoku Electric Power Co., Inc.

4-33, Komachi, Naka-ku, Hiroshima, 730-8701 JAPAN

e Graduate School of Engineering, Hiroshima University

1-4-1 Kagamiyama, Higashi-Hiroshima, Hiroshima 739-8527, Japan

f Faculty of Science & Technology, Ryukoku University

19 1-5 Yokotani, Setaooe, Ootsu, Shiga 520-2194, Japan

20 *Corresponding author:

21 Tel & Fax: +81-78-431-6357, E-mail: s-asaoka@maritime.kobe-u.ac.jp

22 Address: Research Center for Inland Seas, Kobe University, 5-1-1 Fukaeminami,

23 Higashinada, Kobe, 658-0022 JAPAN

24

25

26

27

28

29

30

31

32

33

34

35

36

37 **Highlights**

38 Adsorbent for H₂S was synthesized from mixture of coal ash and blast furnace cement.

39 Mixing ratio of coal ash and blast furnace cement was investigated.

40 H₂S removal rate increased significantly up to 87wt.% of coal ash.

41 The crushing strength was over 1.2 N mm⁻² when the mixing ratio was less than
42 95wt.%.

43 The mixing ratio of coal ash was optimized at 87wt.%.

44

45

46

47

48

49

50

51

52

53

54

55 **Abstract**

56 Reducing hydrogen sulfide concentration in eutrophic marine sediments is crucial to
57 maintaining healthy aquatic ecosystems. Managing fly ash, 750 million tons of which is
58 generated annually throughout the world, is another serious environmental problem. In
59 this study, we develop an approach that addresses both these issues by mixing coal fly
60 ash from coal-fired power plants with blast furnace cement to remediate eutrophic
61 sediments. The purpose of this study is to optimize the mixing ratio of coal fly ash and
62 blast furnace cement to improve the rate of hydrogen sulfide removal based on scientific
63 evidence obtained by removal experiments and XAFS, XRD, BET, and SEM images.
64 In the case of 10 mg-S L⁻¹ of hydrogen sulfide, the highest removal rate of hydrogen
65 sulfide was observed for 87wt.% of coal fly ash due to decreased competition of
66 adsorption between sulfide and hydroxyl ions. Whereas regarding 100 mg-S L⁻¹, the
67 hydrogen sulfide removal rate was the highest for 95wt.% of coal fly ash. However, for
68 both concentrations, the removal rate obtained by 87wt.% and 95wt.% were statistically
69 insignificant. The crushing strength of the mixture was over 1.2 N mm⁻² when the coal
70 fly ash mixing ratio was less than 95wt.%. Consequently, the mixing ratio of coal fly
71 ash was optimized at 87wt.% in terms of achieving both high hydrogen sulfide removal
72 rate and sufficient crushing strength.

73 **Key Words**

74 Coal-fired power plant, Environmental Remediation, Eutrophication, Sediment, Recycle

75

76

77

78

79

80

81

82

83

84

85

86

87

88

89

90

Introduction

The sediments settled in enclosed water bodies, ports, and harbors are affected by significant terrigenous organic matter loads, and the oxidative decomposition of this organic matter consumes dissolved oxygen in the water column. Under such anoxic conditions, hydrogen sulfide is generated by sulfate-reducing bacteria. Investigations of the toxicity of hydrogen sulfide for plants and aquatic organisms (Gray et al, 2002; Lloyd, 2006; Dooley et al., 2013), have reported that it interferes with cytochrome c oxidase, the last enzyme of the electron transport system (Raven and Scrimgeour, 1997; Affonso et al., 2004). Most aquatic organisms are negatively affected by hydrogen sulfide in the range of 2.93-59 μM (Marumo and Yokota, 2012). Generally, high levels of hydrogen sulfide are observed in marine sediments accumulated in enclosed or semi-enclosed water bodies located adjacent to large metropolitan areas and upwelling systems (Azad et al., 2005; Reese et al., 2008; Yamamoto et al., 2012; Sakai et al., 2013; Schunck et al., 2013; Asaoka et al., 2014). Hydrogen sulfide may also cause blue tide and a bad odor when it is upwelling and oxidized through the water column. Therefore, hydrogen sulfide is a significant contributor to the development of oxygen-deficient water masses. One result of this is the reduced viability of benthic organisms and fish, due to hypoxia and the toxicity of hydrogen sulfide. Hence, it is very important to

reduce the hydrogen sulfide concentration of water in order to maintain healthy ecosystems, aquaculture activities, and to protect aquatic environments.

Previous studies have demonstrated that a mixture of coal fly ash (CFA) and blast furnace cement (BFC) called ‘granulated coal ash (GCA)’ adsorbs and oxidizes hydrogen sulfide efficiently (Asaoka et al., 2012; Asaoka et al., 2014). Coal ash is classified into two types: bottom ash generated in boilers and fly ash from a waste gas treatment process, with the latter comprising 85–95% of total coal ash. Annual worldwide generation of fly ash is estimated at approximately 750 million tons (Yao et al., 2015). Even within Japan, 12.5 megatons of coal ash was generated from coal-fired power plants and other industries in 2013 (JCOAL, 2016). In 2011, coal-fired generation accounted for 29.9% of the world electricity supply, and it is estimated that this will increase to 46% by 2030 (Yao et al., 2015). Meanwhile, utilization rates of this fly ash are approximately 70% in China, 65% in India, and 50% in the United States (Yao et al., 2015). Coal ash has been recycled for concrete, road base construction, soil amendment, zeolite synthesis, as an adsorbent, etc (Xie et al., 2013; Xie et al., 2014; Yao et al., 2015). However, these utilization strategies are insufficient for the complete recycling of the increasing amount of coal ash. Therefore, new applications utilizing by-products from coal-fired power plants are expected to contribute to waste reduction and promote

recycling consciousness and within society.

We developed a GCA mix of CFA from coal-fired power plants and BFC in order to remediate eutrophic sediments and found that the GCA successfully removed hydrogen sulfide (Asaoka et al., 2012). When CFA is mixed with cement, the silicon oxide and aluminum oxide contained within it in react with the calcium hydroxide in the BFC. This reaction is called the Pozzolanic reaction (Shi and Day, 2000a; Shi and Day, 2000b); it increases the specific surface area and compression strength of the GCA. Oxidation by manganese oxide on the GCA created a removal mechanism for the hydrogen sulfide (Asaoka et al. 2012). Furthermore, GCA applied to the sediment in enclosed water bodies at a field experiment site suppressed hydrogen sulfide effectively (Asaoka et al., 2014; Asaoka et al., 2015). GCA can simply be scattered or mixed with the organically enriched sediment accumulated in eutrophic areas, such as enclosed water bodies, the innermost areas of bays, lakes, and tidal rivers using a dredging boat to remove hydrogen sulfide (Asaoka et al., 2014; Yamamoto et al, 2015; Nakamoto et al., 2015). Furthermore, the applied GCA in actual filed sites need not be collected because, the adsorption site on the GCA for hydrogen sulfide regenerated through manganese oxidation under oxic conditions such as the vertical mixing seasons (Asaoka et al., 2014). However, mixing ratios of CFA and BFC have not yet been fully clarified

because the present GCA was originally optimized to strengthen construction materials. The purpose of this study was to optimize the mixing ratio of fly ash and BFC to create an environmental remediation agent for the removal of hydrogen sulfide. In this study we will offer solutions for two serious environmental problems—in effect, killing two birds with one stone—namely, utilization of fly ash, and environmental remediation by removing hydrogen sulfide.

Experimental

Preparing the GCA with different ratios of CFA and BFC

The GCAs were prepared by mixing with CFA and BFC. The CFA from coal-fired power plants was provided by the Chugoku Electric Power Co., Inc., Japan. We analyzed the chemical composition of the CFA used in this study by wavelength dispersive X-ray spectrometry (ZSX-100e; Rigaku) with fundamental parameter mode. The CFA was mainly composed of SiO₂ (73.4wt.%), Al₂O₃ (18.1wt.%), Fe₂O₃ (3.01wt.%), CaO (1.40wt.%), K₂O (1.15wt.%), TiO₂ (1.02wt.%), Na₂O (0.42wt.%), SO₃ (0.41 wt.%), MgO (0.31 wt.%), P₂O₅ (0.29 wt.%), V₂O₃ (0.13 wt.%) and other substances. The BFC was also analyzed by wavelength dispersive X-ray spectrometry (Supermini; Rigaku) with fundamental parameter mode. The BFC was mainly

composed of CaO (56.3wt.%), SiO₂ (25.0wt.%), Al₂O₃ (8.90wt.%), SO₃ (3.64wt.%), MgO (2.63wt.%), Fe₂O₃ (1.84wt.%), TiO₂ (0.473wt.%), K₂O (0.424), Na₂O (0.352wt.%), P₂O₅ (0.141wt.%) and other substances.

The CFA was mixed with BFC at a mixing ratio of 0, 40, 70, 87, 95 and 100wt.%. Water was added so that the mixture amounted to 20wt.%. The mixture was then granulated to approximately 5-mm diameter using a rotary pan type granulator. The granulated mixture was then air-dried for at least 10 months in a laboratory to complete the pozzolanic reaction between the CFA and BFC.

Hydrogen sulfide removal experiments

The hydrogen sulfide solution was prepared as follows: Tris-HCl buffer (Kanto Kagaku) was added to 500 mL of pure water deaerated with N₂ gas to a final concentration of 30 mmol L⁻¹. An aliquot of Na₂S•9H₂O (Wako Pure Chemical Industries) was dissolved into the solution. Concentrations of hydrogen sulfide were 10 and 100 mg L⁻¹, to represent the possible range in the pore water of organically enriched sediments. The pH of the solution was adjusted to 8.2, which is the general pH of seawater, by adding HCl or NaOH as necessary.

The batch experiments were conducted in triplicate. Fifty mL of the prepared

hydrogen sulfide solution was slowly dispensed into a 100-mL vial bottle, and 0.2 g of the prepared GCAs was added to the solution. Thereafter, the headspace of the bottle was replaced with N₂ gas. The bottle was plugged with a rubber cork and sealed with an aluminum cap. It was agitated moderately at 100 rpm at 25 °C in a constant-temperature oven, and the time courses of hydrogen sulfide concentration were measured using a detection tube (200SA or 200SB: Komyo Rikagaku Kogyo). The hydrogen sulfide solution was also prepared without the addition of GCAs as a control, and experiments were conducted by the same protocol.

Sulfur K-edge XAFS spectra (ranges 2460-2490 eV) was measured using the BL11 at the Hiroshima Synchrotron Research Center, HiSOR. The synchrotron radiation from a bending magnet was monochromatized with a Si(111) double-crystal monochromator. The sample chamber was filled with He gas, and XAFS spectra were measured by X-ray fluorescence yield mode using a SDD detector (XR-100SDD; AMPTEK). The K-edge main peak of sulfate derived from CuSO₄ • 5H₂O was set to 2481.6 eV. The pieces of relatively flat GCAs with adsorbed hydrogen sulfide were mounted on double-stick tape (NW-K15; Nichiban) and placed in the central hole (15-mm diameter) of a copper plate. The surface of the sample was attached to that of the copper plate. The angle between the incident X-ray and the sample surface was adjusted at 20°, and the

X-ray fluorescence was detected from the direction normal to the incident beam in the plane of the electron orbit of the storage ring.

As references, $\text{CuSO}_4 \cdot 5\text{H}_2\text{O}$ (Wako Pure Chemical Industry) represents sulfate and sulfur (Wako Pure Chemical Industry) were also measured by the conversion electron yield mode.

Physicochemical properties of the GCAs

The specific surface area of the GCA and fly ash used in this study was determined by the Brunauer-Emmett-Teller method (nitrogen gas adsorption) using surface area and pore size analyzers (ASAP2020; Micromeritics).

The SEM photo on the GCA was taken by a scanning electron microscope (JXA-8200; JEOL). The GCA was mounted on a carbon tape and deposited by carbon vapor. The secondary electron images of the flat surface of the GCAs were taken at an accelerating voltage of 15.0 kV.

A compact water quality meter (LAQUA twin pH; HORIBA) was used to measure the surface pH of the GCAs. A CMF filter sheet (Y100A13; Advantec) was installed on the electrode, and a GCA particle was placed on the filter. A few drops of ultrapure water were then dripped onto the GCA particle to measure the surface pH of the GCA.

A compression tester (LD-01D; Shinohara) was used to measure the crushing strength of the GCAs.

The powder X-ray diffraction pattern of the GCAs was measured by an X-ray diffractometer (RAD-RU300; Rigaku). The CGAs were exposed to the X-ray beam from Co-K α radiation at 40 kV and 200 mA. The scanning range of the diffraction angle 2θ was 5°-90° at 0.02-step intervals and a scan rate of 2° min⁻¹. The crystalline materials in the GCAs were semi-quantified by the reference intensity ratio method using a crystallography database (PDXL; Rigaku).

The percentage of the pozzolanic reaction P (wt.%) was calculated by Eq. 1.

$$P(\text{wt. \%}) = \left(\frac{W_i - W_g}{W_i} \right) \cdot 100, \quad (1)$$

where W_i and W_g were the total weight of pozzolan in CFA and BFC, and the weight of pozzolan in the GCAs, respectively.

The weight of pozzolan was determined by following procedure (Kano et al., 2002). One gram of the powdered GCA sample was added to 200 mL of ultrapure water kept at pH 2 by adding 1 mol L⁻¹ HCl, and stirred for 20 min. The GCA was then entrapped by a quantitative filter paper (Ashless Grades, No. 40; Whatman) and transferred to a

ceramic crucible. The entrapped GCA in the ceramic crucible was heated in an electric furnace at 1000 °C for 30 min. The weight of the residue was defined as the pozolan.

Results and discussion

Removal kinetics of hydrogen sulfide by the GCA

The removal kinetics of hydrogen sulfide is well-expressed as the first-order equation described by Eq. 2 (**Figs. 1a and 1b**).

$$[C_t] = [C_0]e^{-kt} \quad (2)$$

where $[C_t]$: concentration of hydrogen sulfide at time t (mg-S L⁻¹), $[C_0]$: initial concentration of hydrogen sulfide (mg-S L⁻¹), t : time (h), and k : first order rate constant (h⁻¹).

The removal rate constants obtained by this study are shown in **Table 1**. In the controls without the GCA, the concentration of hydrogen sulfide decreased slightly due to oxidation and volatilization. On the other hand, the concentration of hydrogen sulfide decreased significantly with addition of the GCAs. In the case of initial concentration at 10 mg-S L⁻¹, the removal rates of hydrogen sulfide of all the GCAs were higher

compared to the control (ANOVA; $p < 0.01$) (**Table 1**). The addition of CFA to the BFC increased hydrogen sulfide removal rate significantly compared to no CFA (ANOVA; $p < 0.01$). The removal rate of hydrogen sulfide obtained by the GCA contained in 87wt.% of CFA was significantly higher than that of other GCAs (0, 40 and 70wt.% of CFA; ANOVA; $p < 0.01-0.05$). The mixing ratio of CFA beyond 87wt.% did not show significant increase in hydrogen sulfide removal rate (ANOVA; $p = 0.222$ between 87wt.% and 95wt.%). Hence, the highest hydrogen sulfide removal rate was found at 87wt.% of CFA.

In the case of initial concentration at 100 mg-S L^{-1} , the hydrogen sulfide removal rate for all GCAs were also higher compared to the control (ANOVA; $p < 0.01$) (**Table 1**). When the mixing ratio of CFA exceeded 87wt.%, the removal rates of hydrogen sulfide were significantly increased (ANOVA; $p < 0.01$). The hydrogen sulfide removal rate was the highest for 95wt.% of coal fly ash. The hydrogen sulfide was removed completely within 3 days by the GCA with 95wt% of CFA. Therefore, the GCA with 95wt% of CFA could not be plotted after 72 h in **Fig. 1b**. However, the removal rate obtained by 87wt.% and 95wt.% were statistically insignificant (ANOVA; $p = 0.157$).

The sulfur K-edge spectra of the GCAs after adsorption of hydrogen sulfide (initial concentration: 100 mg-S L^{-1}) are shown in **Fig. 2**. A peak at 2482 eV indicates that

sulfate was mainly derived from fly ash (Asaoka et al., 2012). The peak around 2472 eV represents sulfur. The sulfur peak at 2472 eV was not identified on the BFC, i.e., GCA with 0wt.% of CFA. Meanwhile, the sulfur peaks on the GCAs were increased by the increase of the mixing ratio of the CFA, corresponding to the increase in the hydrogen sulfide removal rate. A previous study demonstrated that hydrogen sulfide was oxidized to sulfur on the surface of the GCA (Asaoka et al., 2012); given that, we found that oxidation rate to sulfur from hydrogen sulfide was increased by increasing the mixing ratio of CFA. Oxidation rate was also increased by the raising the removal amount of hydrogen sulfide corresponding to the increase of the CFA mixing ratio. The amount of hydrogen sulfide removed at each the GCAs ratios after 72 h were 2.1, 5.0, 5.0, 9.8 and 15 mg g⁻¹ for 0, 40, 70, 87 and 95wt.% of CFA addition, respectively (**Table 1**).

Physicochemical properties of the GCAs

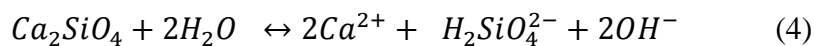
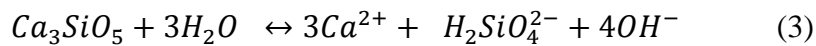
The physicochemical properties of the GCAs are shown in **Table 2**. The major parameters controlling the removal rate of hydrogen sulfide are considered to be specific surface area, surface pH, and manganese content originated from the CFA. The specific surface area reached a maximum at GCAs of 70wt.% of CFA; correspondingly, the pozzolanic reaction percentage also reached its maximum at this mixing ratio. The

specific surface area of the CFA was initially $2 \text{ m}^2 \text{ g}^{-1}$. Therefore, the pozzolanic reaction made the structure of the GCAs porous. There is a positive relation between CFA content in the GCAs and the removal rate of hydrogen sulfide ($r=0.9574$ and 0.8431 for initial concentrations of hydrogen sulfide of 10 and 100 mg-S L^{-1} , respectively; **Fig. S1**); this is supported by the hydrogen sulfide oxidizing to sulfur by the manganese oxide from CFA (Asaoka et al., 2012). In contrast, the removal rate of hydrogen sulfide is negatively correlated with the surface pH of the GCAs ($r=0.9232$ and 0.9143 for initial concentrations of hydrogen sulfide 10 and 100 mg-S L^{-1} , respectively; **Fig. 3**). This was attributed to competitive adsorption between HS^- or S^{2-} and OH^- . For example, dissociation of 10 mg L^{-1} of hydrogen sulfide at each pH was calculated using a chemical equilibrium model software, Visual MINTEQ ver.3.0 (**Fig. 4**). The concentration of S^{2-} is much lower than that of OH^- in the range of pH 1-14. However, when the pH is above 10.4, the concentration of OH^- becomes higher than that of HS^- . Therefore, the competitive adsorption between HS^- and OH^- decreases the removal rate of hydrogen sulfide. The competitive adsorption on the GCAs with 87 and 95wt.% of CFA might be less than that of other GCAs because the surface pH of those GCAs was lower than that of other GCAs. Hence the removal rate of hydrogen sulfide obtained by the GCAs with 87 and 95wt.% of CFA was much higher than that of other

GCA.s.

One of the factors in controlling surface pH is the mineral composition of the GCAs. The mineral composition of the GCAs is shown in **Fig. 5**. The GCAs was mainly composed of quartz (ICDD46-1045; SiO₂), mullite (ICDD15-0776; Al₆Si₂O₁₃), tricalcium silicate (ICDD86-0402; Ca₃SiO₅), dicalcium silicate (ICDD83-0461 and ICDD24-0034; Ca₂SiO₄) and calcite (ICDD05-0586; CaCO₃). Mullite and quartz originate mainly from fly ash (Criado et al, 2007). On the other hand, Ca₃SiO₅ and Ca₂SiO₄, corresponding to tricalcium silicate and dicalcium silicate, come from BFC (Wang and Vipulanadan, 2000; Marques et al., 2006). The composition ratio of tricalcium silicate and dicalcium silicate in the GCA with 70wt.% of CFA was highest in the GCAs with 40–90wt.% of CFA, which corresponds to the pozzolanic reaction percentage of the GCA that was also the highest (70wt.% of CFA).

The dissolution reactions for Ca₃SiO₅ and Ca₂SiO₄ were assumed to be Eqs. 3 and 4, respectively (Garrault and Nonat, 2001; Bullard and Flatt, 2010).



According to Eqs. 3 and 4, the OH^- that contributes to the increase of the surface pH on the GCAs is generated by the dissolution of Ca_3SiO_5 and Ca_2SiO_4 . These calcium silicates account for a large percentage of the GCAs with 0–70wt.% of CFA, compared to those with 87 and 95wt.% of CFA. Therefore, the surface pH of the GCAs with 0–70wt.% fly ash was higher than those with 87 and 95wt.% of CFA.

In short, the results suggest that GCAs with 87 and 95wt.% of CFA are good candidates for hydrogen sulfide removal. Another important factor is the crushing strength of the GCAs. The GCAs require over 1.2 N mm^{-2} crushing strength to withstand the weight and strain of the heavy machinery used for environmental remediation. The crushing strength of the GCAs is shown in **Table 2**. The crushing strength increased with decreasing mixing ratio of coal ash. Thus, a negative correlation was observed between the crushing strength and the mixing ratio of coal ash ($r=0.9953$; **Fig. 6**). In contrast, a positive correlation was observed between the percentage of amorphous in the GCAs and the mixing ratio of coal ash ($r=0.9902$; **Fig. S2**). From these two correlations, the crushing strength of the GCAs could be controlled by crystallinity. The crushing strength of the GCAs reached over 1.2 N mm^{-2} when the fly ash mixing ratio was less than 95wt.%. SEM images of the GCAs with 87wt.% and 95wt.% of CFA are shown in **Figs. S3a and S3b**, respectively. In the case of the GCA

with 95wt.% of CFA, CFA sphere particles were observed (**Fig. S3b**). Meanwhile, the new crystal phase formed by the pozzolanic reaction filled in the space between the fly ash particles in GCA with 87wt.% of GCA (**Fig. S3a**).

Conclusions

This study investigated the optimum mixing ratio of coal fly ash (CFA) and blast furnace cement (BFC) to produce the granulated coal ash (GCA). When the mixing ratio of CFA up to 87wt.%, the rate of hydrogen sulfide removal increased significantly due to decreased competition of adsorption between sulfide and hydroxyl ions. The OH⁻ attributed to dissolution of calcium silicate on the surface of the GCAs containing 87 and 95wt.% of CFA was considered to be low compared to the other GCAs. Moreover, the crushing strength of the GCA containing 95wt.% CFA was lower than 1.2 N mm⁻² because the most of crystal phase of the GCA was amorphous. Consequently, the optimum mixing ratio of CFA and BFC to produce the GCA was 87 wt.% and 13 wt.% in terms of achieving both a high hydrogen sulfide removal rate and sufficient crushing strength.

Acknowledgements

This study was partially supported by the Japan Society for the Promotion of Science JSPS KAKENHI Grant B25740038.

XAFS analyses at the Hiroshima Synchrotron Radiation Center, Hiroshima University, were carried out under the approval of the Project for Collaborative Research (14-A-2).

References

- Affonso, E.G., Polez, V. L. P., Corrêa, C. F., Mazon, A. F., Araújo, M. R. R., Moraes, G., Rantin, F. T. 2004., Physiological responses to sulfide toxicity by the air-breathing catfish, *Hoplosternum littorale* (Siluriformes, Callichthyidae). *Comp. Biochem. Physiol., C.*, 139(4), 251-257, DOI 10.1016/j.cca.2004.11.007.
- Asaoka, S., Hayakawa, S., Kim, K. H., Takeda, K., Katayama, M., Yamamoto, T., 2012. Combined adsorption and oxidation mechanisms of hydrogen sulfide on granulated coal ash. *J. Colloid Interf. Sci.*, 377, 284-290, DOI 10.1016/j.jcis.2012.03.023.
- Asaoka, S., Okamura, H. Akita, Y., Nakano, K., Nakamoto, K., Hino, K., Saito, T., Hayakawa, S., Katayama, M., Inada, Y., 2014. Regeneration of manganese oxide as

adsorption sites for hydrogen sulfide on granulated coal ash. Chem. Eng. J., 254,
531-537, DOI 10.1016/j.cej.2014.06.005.

Asaoka, S., Yamamoto, T., Yamamoto, H., Okamura, H., Hino, K., Nakamoto, K.,
Saito, T., 2015. Estimation of hydrogen sulfide removal efficiency with granulated
coal ash applied to eutrophic marine sediment using a simplified simulation
model. Mar. Pollut. Bull., 94(1-2), 55-61, DOI 10.1016/j.marpolbul.2015.03.017.

Azad, M.A.K., Ohira, S., Oda, M., Toda, K., 2005. On-site measurements of hydrogen
sulfide and sulfur dioxide emissions from tidal flat sediments of Ariake Sea, Japan.
Atmos. Environ., 39(33), 6077-6087, DOI 10.1016/j.atmosenv.2005.06.042.

Bullard, J. W., Flatt, R. J., 2010. New insights into the effect of calcium hydroxide
precipitation on the kinetics of tricalcium silicate hydration. J. Am. Ceram. Soc.,
93(7), 1894-1903, DOI 10.1111/j.1551-2916.2010.03656.x.

Criado, M., Fernandez-Jimenez, A., de la Torre, A. G., Aranda, M. A. G., Palomo, A.,
2007. An XRD study of the effect of the $\text{SiO}_2/\text{Na}_2\text{O}$ ratio on the alkali activation
of fly ash. Cem. Concr. Res., 37(5), 671-679, DOI
10.1016/j.cemconres.2007.01.013.

Dooley, F. D., Wyllie-Echeverria S., Roth M. B., Ward P. D., 2013. Tolerance and
response of *Zostera marina* seedlings to hydrogen sulfide. Aquatic Botany., 105,

397 7-10, DOI 10.1016/j.aquabot.2012.10.007

398 Garrault, S., Nonat, A., 2001. Hydrated layer formation on tricalcium and dicalcium
399 silicate surfaces: Experimental study and numerical simulations. *Langmuir*,
400 17(26), 8131-8138, DOI 10.1021/la011201z.

401 Gray, J. S., Wu, R. S. S., Or, Y. Y., 2002. Effects of hypoxia and organic enrichment on
402 the coastal marine environment. *Mar. Ecol. Prog. Ser.*, 238, 249-279, DOI
403 10.3354/meps238249.

404 JCOAL Website, <http://www.jcoal.or.jp/coaldb/tech/coalash/> (Accessed on September
405 30, 2016)

406 Kano, K., Akiyama T., Matsui J., Ikabata, T., 2002. Phase composition and porosity of
407 low heat portland cement with large amount of pozzolan. *Cem. Sci. Conc.*
408 *Technol.*, 55, 75-82 (in Japanese with English abstract)

409 Lloyd, D., 2006. Hydrogen sulfide: clandestine microbial messenger? *Trends*
410 *Microbiol.*, 14(10), 456-462, DOI 10.1016/j.tim.2006.08.003.

411 Marques, S. F., Ribeiro, R. A., Silva, L. M., Ferreira, V. M., Labrincha, J. A., 2006.
412 Study of rehabilitation mortars: Construction of a knowledge correlation matrix.
413 *Cem. Concr. Res.*, 36(10), 1894-1902, DOI 10.1016/j.cemconres.2006.06.005.

414 Marumo, K., Yokota, M., 2012. Review on Aoshio and biological effects of hydrogen

415 sulfide. Rep. Mar. Ecol. Res. Inst., 15, 23-40. (in Japanese).

416 Nakamoto, K., Hibino T., Hino K., Touch N., 2015. Granulated Coal Ash – used
417 method for remediation of organic matter enriched coastal sediments. Proc. Eng.,
418 116, 326-333, DOI 10.1016/j.proeng.2015.08.297

419 Raven, J.A., Scrimgeour, C.M., 1997. The influence of anoxia on plants of saline
420 habitats with special reference to the sulphur cycle. Annal. Bot., 79, 79–86.

421 Reese, B.K., Anderson, M.A., Amrhein, C., 2008. Hydrogen sulfide production and
422 volatilization in a polymictic eutrophic saline lake, Salton Sea, California. Sci.
423 Total Environ., 406(1-2), 205-218, DOI 10.1016/j.scitotenv.2008.07.021.

424 Sakai, S., Nakaya, M., Sampei, Y., Dettman, D.L., Takayasu, K., 2013. Hydrogen
425 sulfide and organic carbon at the sediment–water interface in coastal brackish
426 Lake Nakaumi, SW Japan. Environ. Earth Sci., 68(7), 1999-2006, DOI
427 10.1007/s12665-012-1887-5.

428 Schunck, H., Lavik, G., Desai, D. K., Grosskopf, T., Kalvelage, T., Loscher, C. R.,
429 Paulmier, A., Contreras, S., Siegel, H., Holtappels, M., Rosenstiel, P., Schilhabel,
430 M. B., Graco, M., Schmitz, R. A., Kuypers, M. M. M., LaRoche, J., 2013. Giant
431 hydrogen sulfide plume in the oxygen minimum zone off Peru supports
432 chemolithoautotrophy. PLOS ONE, 8(8), e68661, DOI

433 10.1371/journal.pone.0068661.

434 Shi, C., Day, R. L., 2000a. Pozzolanic reaction in the presence of chemical activators
435 Part I. Reaction kinetics. Cem. Concr. Res., 30(1), 51-58, DOI
436 10.1016/S0008-8846(99)00205-7.

437 Shi, C., Day, R. L., 2000b. Pozzolanic reaction in the presence of chemical activators
438 Part II. Reaction products and mechanism. Cem. Concr. Res., 30(4), 607-613,
439 DOI 10.1016/S0008-8846(00)00214-3.

440 Wang, S., Vipulanadan, C., 2000. Solidification/stabilization of Cr(VI) with cement
441 leachability and XRD analyses. Cem. Concr. Res., 30(3), 385-389, DOI
442 10.1016/S0008-8846(99)00265-3.

443 Xie, J., Wang, Z., Wu, D. Y., Zhang, Z. J., Kong, H. N., 2013. Synthesis of
444 zeolite/aluminum oxide hydrate from coal fly ash: A new type of adsorbent for
445 simultaneous removal of cationic and anionic pollutants. Ind. Eng. Chem. Res.,
446 52(42), 14890-14897, DOI 10.1021/ie4021396.

447 Xie, J., Wang, Z., Wu, D. Y., Kong, H. N. 2014. Synthesis and properties of
448 zeolite/hydrated iron oxide composite from coal fly ash as efficient adsorbent to
449 simultaneously retain cationic and anionic pollutants from water. Fuel, 116,
450 71-76, DOI 10.1016/j.fuel.2013.07.126.

451 Yamamoto, T., Kondo, S., Kim, K. H., Asaoka, S., Yamamoto, H., Tokuoka, M.,
452 Hibino, T., 2012. Remediation of muddy tidal flat sediments using hot air-dried
453 crushed oyster shells. Mar. Pollut. Bull., 64(11), 2428-2434, DOI
454 10.1016/j.marpolbul.2012.08.002.

455 Yamamoto, T., Kim, K. H., Shirono, K., 2015. A pilot study on remediation of
456 sediments enriched by oyster farming wastes using granulated coal ash. Mar.
457 Pollut. Bull., 90(1-2), 54-59, DOI 10.1016/j.marpolbul.2014.11.022

458 Yao, Z. T., Ji, X.S., Sarker, P. K., Tang, J. H., Ge, L. Q., Xia, M. S., Xi, Y. Q., 2015.
459 A comprehensive review on the applications of coal fly ash. Earth Sci. Rev., 141,
460 105-121, DOI 10.1016/j.earscirev.2014.11.016.

461

Figure captions

Fig. 1 Removal kinetics of hydrogen sulfide by GCAs

(a) and (b) are initial concentrations of 10 and 100 mg-S L⁻¹, respectively

Fig. 2 The Sulfur K edge spectra of the GCAs after adsorption of hydrogen sulfide

Fig. 3 The relationship between the surface pH of GCAs and removal rate of hydrogen sulfide

Fig. 4 The concentration of sulfide species as a function of pH

Fig. 5 The mineral composition of GCAs determined by XRD

Fig. 6 The relationship between the coal fly ash mixing ratio of GCAs and crushing strength of the GCAs

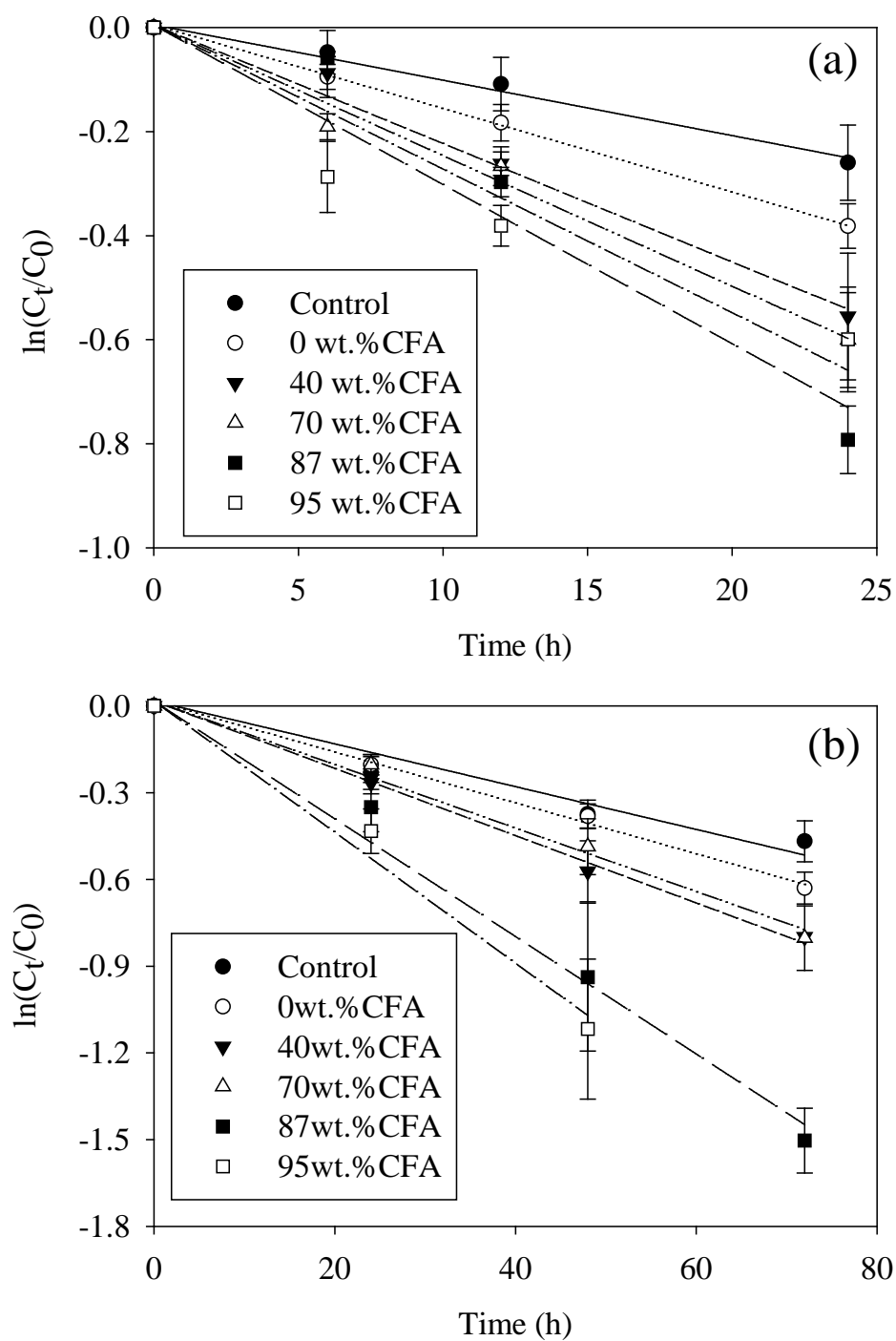


Fig. 1 Removal kinetics of hydrogen sulfide by GCA

(a) and (b) are initial concentrations of 10 and 100 mg-S L⁻¹, respectively

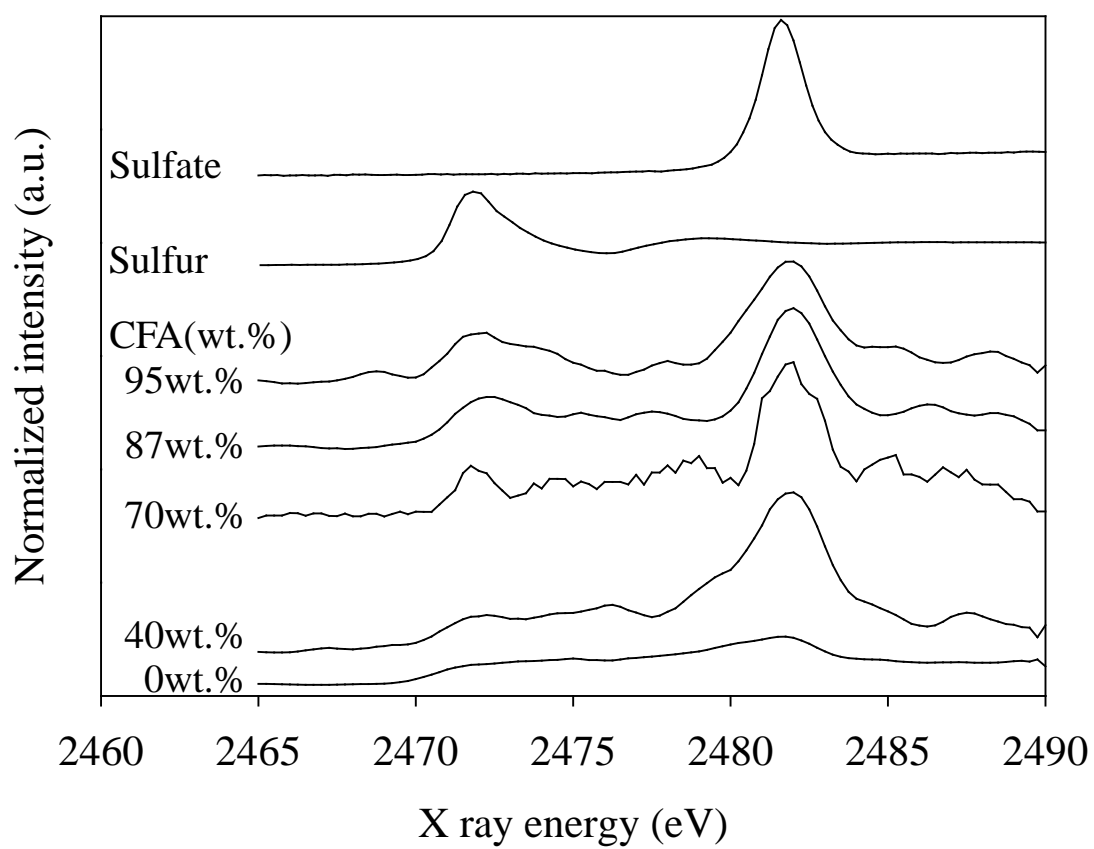


Fig. 2 The Sulfur K edge spectra of the GCAs after adsorption of hydrogen sulfide

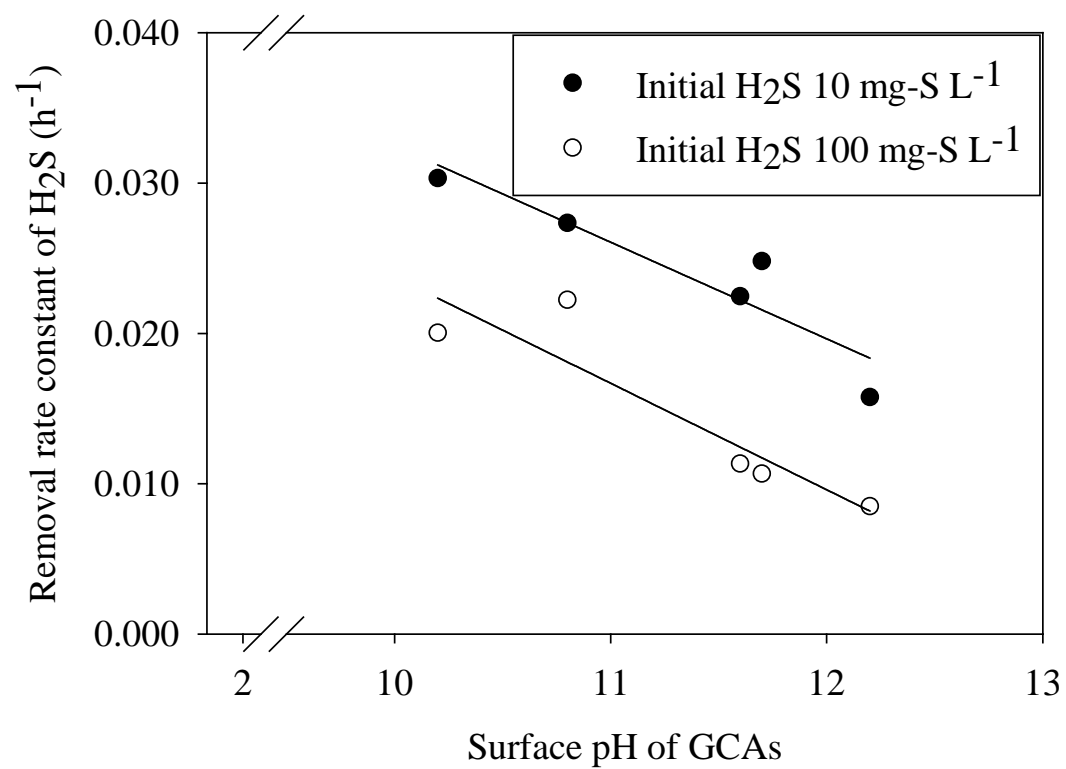


Fig. 3 The relationship between the surface pH of GCAs and removal rate of hydrogen sulfide

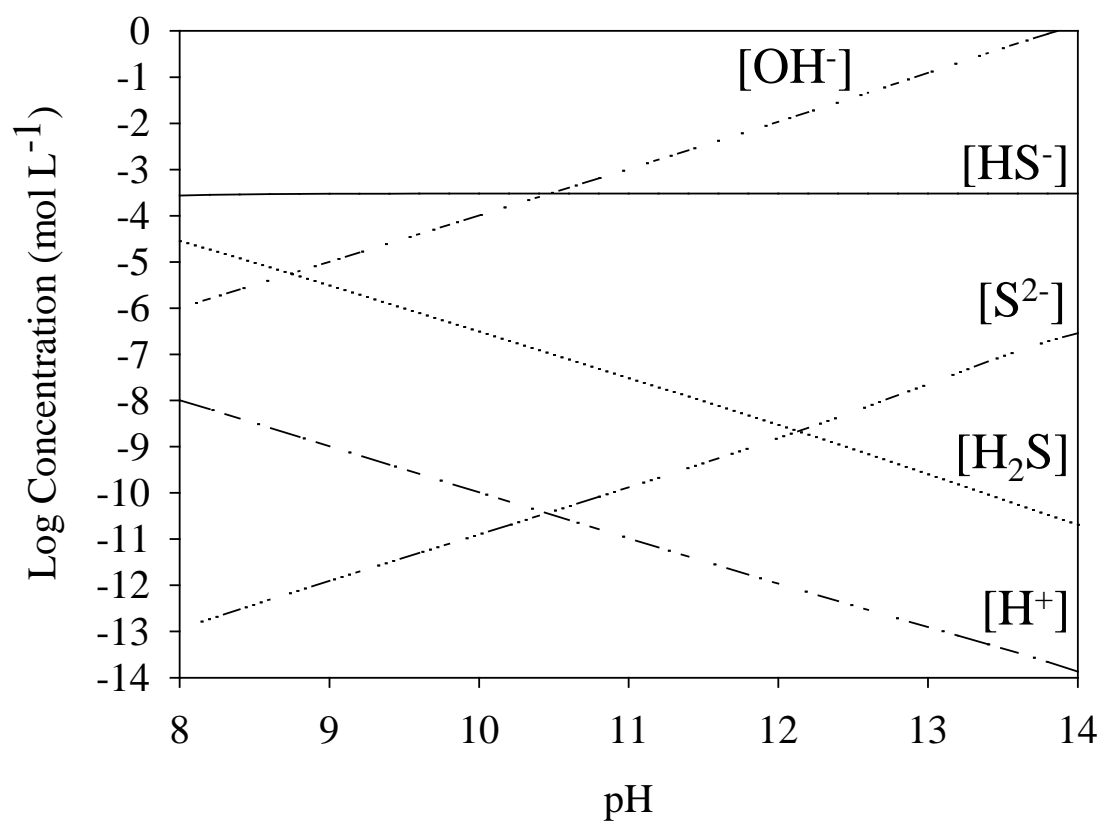


Fig. 4 Concentration of sulfide species as a function of pH

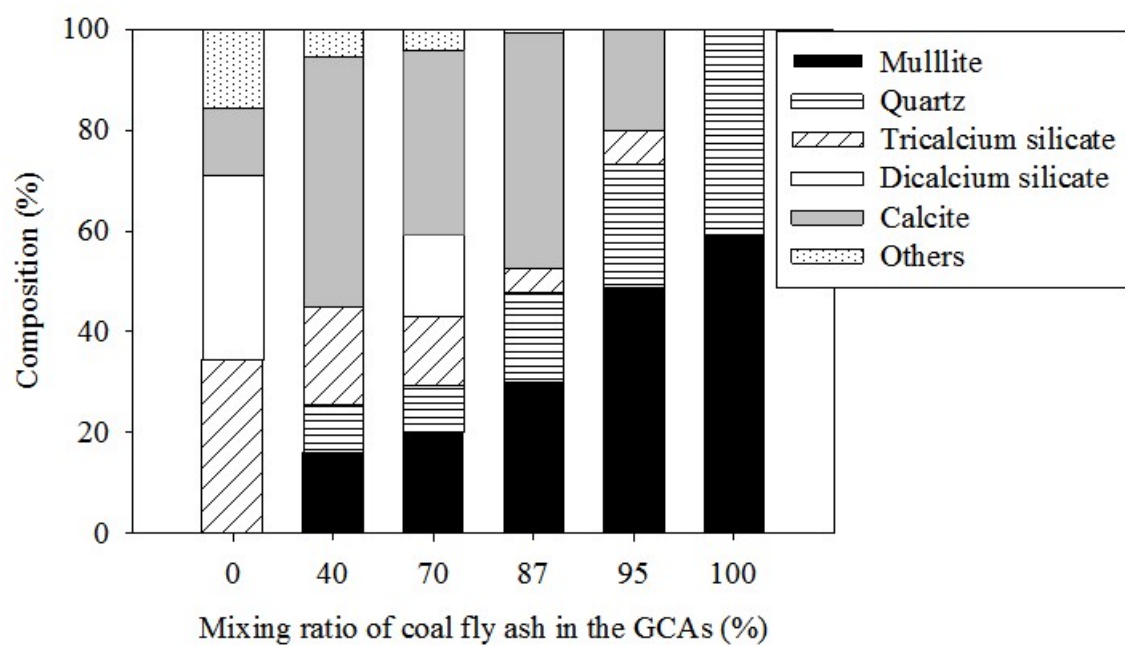


Fig. 5 The mineral composition of the GCAs as determined by XRD

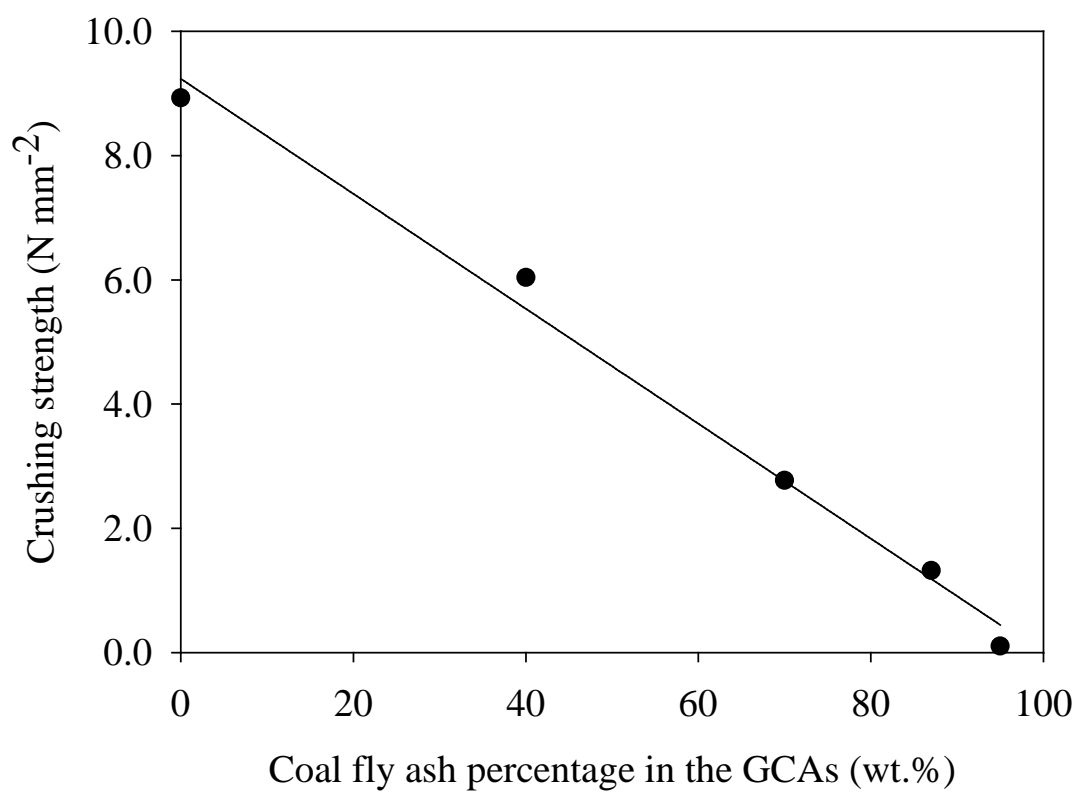


Fig. 6 The relationship between the coal fly ash mixing ratio of GCAs and crushing strength of the GCAs

Table 1 Removal rate and amount of hydrogen sulfide by the GCAs

		Initial H ₂ S concentration (10 mg-S L ⁻¹)			Initial H ₂ S concentration (100 mg-S L ⁻¹)		
		Rate constant; k (h ⁻¹)±SD	r	Removal (mg g ⁻¹) ±SD	Rate constant; k (h ⁻¹)±SD	r	Removal (mg g ⁻¹) ±SD
Control		0.010±0.003	0.992	-	0.0071±0.0009	0.973	-
CFA	95wt.%	0.027±0.003	0.941	0.58±0.13	0.022±0.004	0.990	15±0
CFA	87wt.%	0.030±0.003	0.969	0.99±0.07	0.020±0.003	0.992	9.8±0.6
CFA	70wt.%	0.025±0.003	0.993	0.43±0.13	0.011±0.0007	0.994	5.0±1.3
CFA	40wt.%	0.023±0.004	0.993	0.43±0.17	0.011±0.0007	0.998	5.0±0
CFA	0wt.%	0.016±0.001	1.000	0.23±0.07	0.0085±0.0006	0.998	2.1±0.7

SD is standard deviation in triplicate and r is correlation coefficient of the fitting by the first order kinetics. Removal stands for removal amount of hydrogen sulfide after 24 h or 72 h for initial concentrations of 10 or 100 mg-S L⁻¹, respectively.

Table 2 Physicochemical properties of the GCAs

CFA (wt.%)	Specific surface area (m ² g ⁻¹)	Surface pH	Crushing strength (N mm ⁻²)	Pozzolanic reaction (%)	Amorphous (%)	MnO from CFA (mg kg ⁻¹)
95	8.53	10.8	0.102	2.8	61.8	360
87	11.4	10.2	1.32	8.1	61.2	330
70	20.8	11.7	2.77	15	54.5	260
40	7.44	11.6	6.04	10	48.8	150
0	7.70	12.2	8.93	n.d.	41.6	0

n.d.: not determined. MnO concentration was calculated from CFA mixing ratio.

Supporting information

Optimum reaction ratio of coal fly ash to blast furnace cement for effective removal
of hydrogen sulfide

Satoshi ASAOKA^{a*}, Hideo OKAMURA^a, Kyunghoi KIM^b,
Yuzuru HATANAKA^c, Kenji NAKAMOTO^d, Kazutoshi HINO^d,
Takahito OIKAWA^d, Shinjiro HAYAKAWA^e, Tetsuji OKUDA^f

^a Research Center for Inland Seas, Kobe University

5-1-1 Fukaeminami, Higashinada, Kobe, 658-0022 JAPAN

^b College of Environmental and Marine Sciences and Technology, Pukyong National University

45, Yongso-ro, Nam-Gu, Busan 48513, KOREA

^c Faculty of Maritime Sciences, Kobe University

5-1-1 Fukaeminami, Higashinada, Kobe, 658-0022 JAPAN

^d The Chugoku Electric Power Co., Inc.

4-33, Komachi, Naka-ku, Hiroshima, 730-8701 JAPAN

^e Graduate School of Engineering, Hiroshima University

1-4-1 Kagamiyama, Higashi-Hiroshima, Hiroshima 739-8527, Japan

^f Faculty of Science & Technology, Ryukoku University

1-5 Yokotani, Setaooe, Ootsu, Shiga 520-2194, Japan

*Corresponding author:

Tel & Fax: +81-78-431-6357, E-mail: s-asaoka@maritime.kobe-u.ac.jp

Address: Research Center for Inland Seas, Kobe University, 5-1-1 Fukaeminami, Higashinada,
Kobe, 658-0022 JAPAN

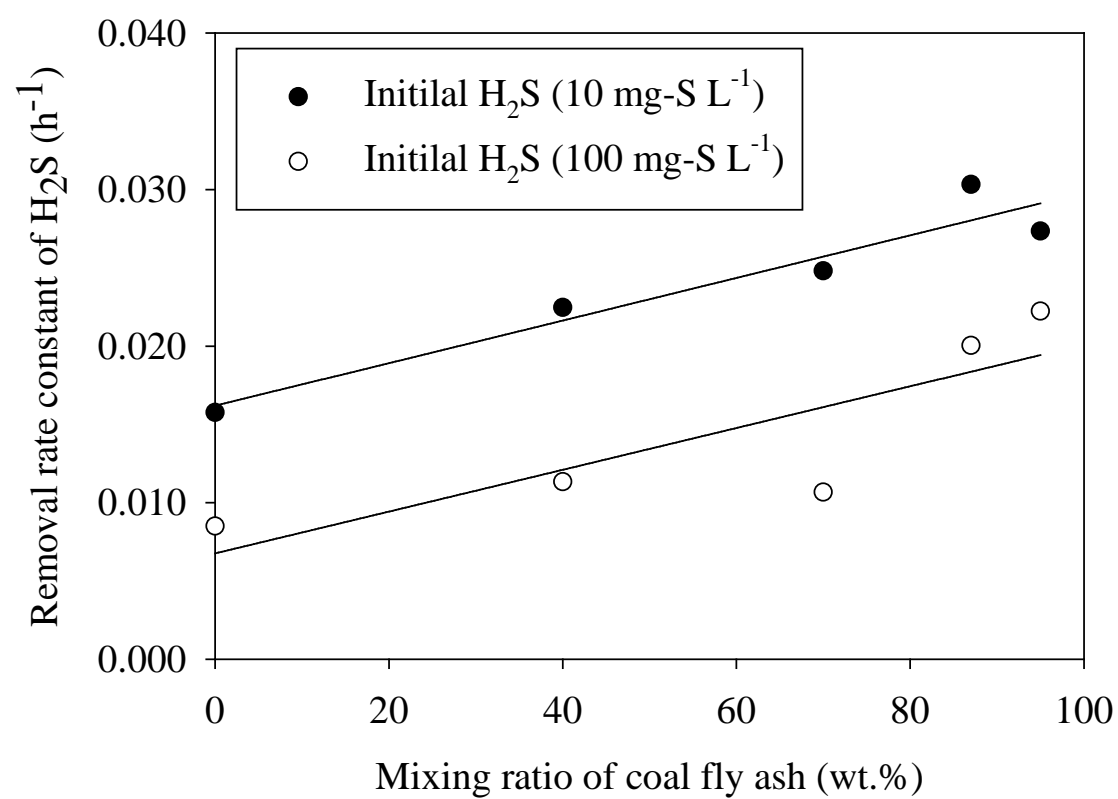


Fig. S1 The relationship between coal fly ash content in the GCAs and removal rate of hydrogen sulfide

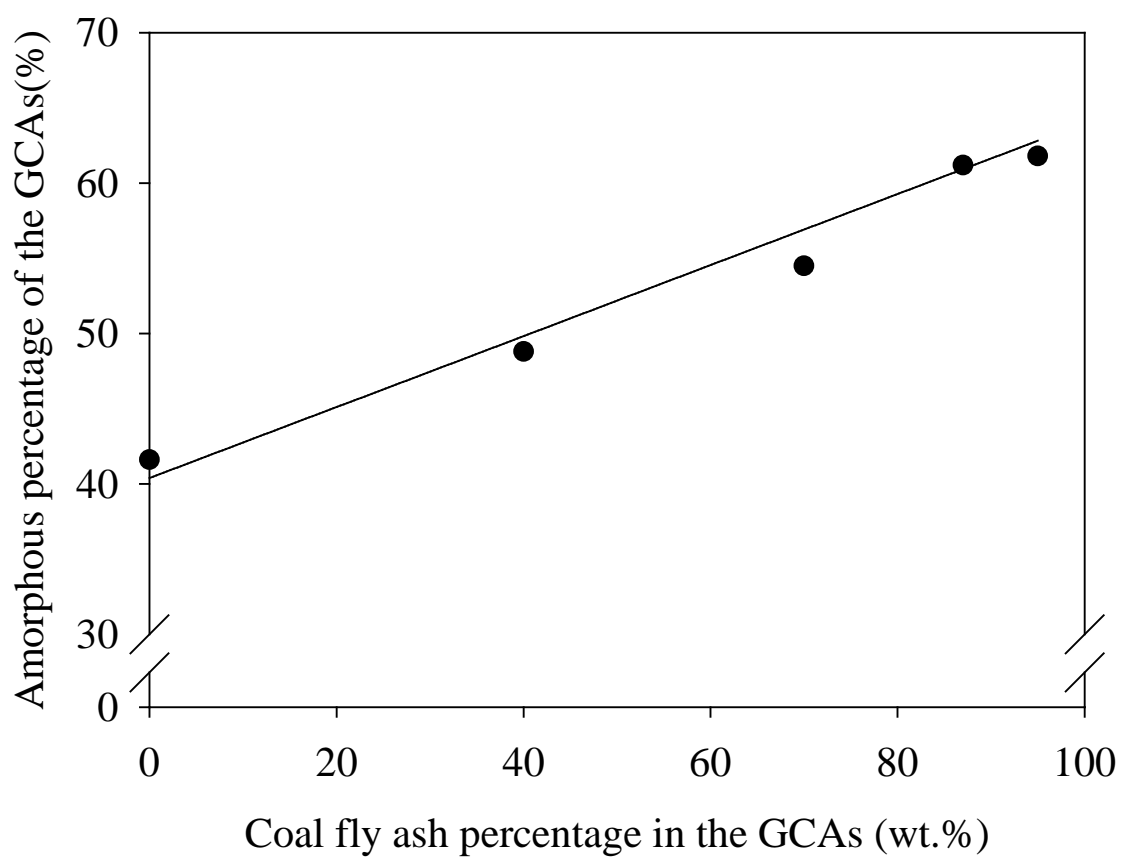


Fig. S2 The relationship between the coal fly ash mixing ratio of the GCAs and amorphous percentage of GCAs

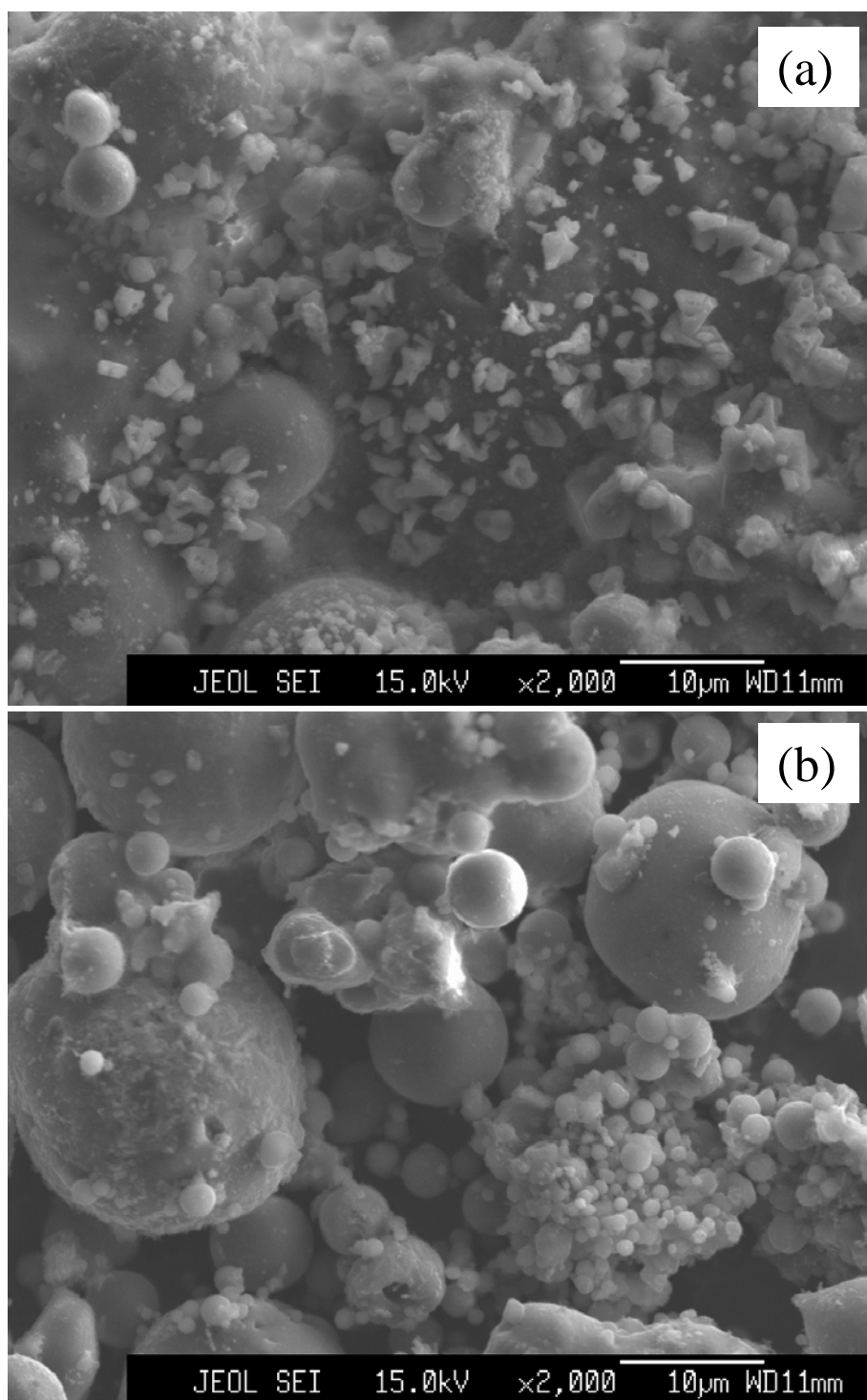


Fig. S3 SEM images of the GCAs with 87wt.% (a) and 95wt.% (b) of CFA

Highlights

Adsorbent for H₂S was synthesized from mixture of coal ash and blast furnace cement.

Mixing ratio of coal ash and blast furnace cement was investigated.

H₂S removal rate increased significantly up to 87wt.% of coal ash.

The crushing strength was over 1.2 N mm⁻² when the mixing ratio was less than 95wt.%.

The mixing ratio of coal ash was optimized at 87wt.%.